16th ICAAR LISBOA 2020-2022

16th International Conference on
Alkali-Aggregate Reaction in Concrete
Lisboa | LNEC | Portugal | 31 May - 2 June 2022

http://icaar2020-2022.lnec.pt

About the colloidal nature of ASR products

Colin Giebson [(1)]

(1) *Bauhaus-University, Weimar, Germany, colin.giebson@uni-weimar.de*

Abstract

The alkali-silica reaction (ASR) generates a product from which is assumed to absorb water and build up swelling pressures in aggregates and the cement paste, resulting in expansion and cracking of concrete. However, studies showed that ASR products often have a crystalline structure and absorb less water than expected. In addition, measured swelling pressures are often surprisingly low. Apparently, the nature of ASR products is not yet sufficiently well understood.

A couple of recent observations showed that ASR products could be considered as colloidal systems, i.e. as a state of finely divided matter dispersed in a medium. In order to clarify, if and to what extent ASR products exhibit colloidal properties, 10 ASR products of different composition and water content have been synthesized at two temperatures (40 and 60 °C) and are currently under investigation. Among other methods, the ASR products are studied at different ages with the cryo-SEM technique, nanoparticle tracking analysis and by means of an osmotic cell test. First results show that ASR products contain particles of colloidal size, mainly between 50-600 nm. There is evidence for an ageing process, resulting in a change of particle size and number as well as in the formation of fractal-like structures. Most important, the ASR products free of Ca show the DONNAN effect, caused by the colloidal particles and resulting in osmosis.

Keywords: *ASR products; colloidal particles; DONNAN effect; osmosis*

1. INTRODUCTION

Recently, silica dissolution rates and properties of synthetic ASR products were determined for the simulation of ASR induced expansion and damage [1, 2]. During the investigations, the following observations were made that initiated a subsequent study:

- Measured swelling pressures of ASR products with Ca were surprisingly low (≤ 2 MPa)
- The initial water content of the ASR products highly influenced their swelling capacity
- ASR products rich in Si and free of Ca did not pass filters with a pore size of ≤ 200 nm
- ASR products free of Ca showed the TYNDALL effect (light scattering)

The latter two observations are typical for colloidal systems and opened up a new perspective on ASR products. Nearly 100 years before ASR in concrete was discovered in the 1930s, colloids and particularly silica gels were begun to be studied by BERZELIUS (1833), later more extensively by GRAHAM (1862), VAN BEMMELEN (1888), ZSIGMONDY (1905) and some others [3]. Based on their work, silica gels can be understood as colloids, i.e. as systems of dispersed particles with a size of 1 to 1000 nm distributed in a dispersion medium. Because of the high surface of the particles, surface-related properties dominate over solid-state properties. Important features of colloids are (1) the continuous BROWNian motion of its particles, (2) the scattering of light by the particles, known as the TYNDALL effect, (3) the DONNAN effect, a special form of osmosis, (4) electrophoresis, (5) OSTWALD ripening, the growth of larger particles from those of smaller size, (6) aggregation and crystallisation [3, 4]. It is the objective of this study to clarify, if and to what extent ASR products show those properties and whether this could help to better understand their nature and the mechanism of swelling and expansion in concrete.

Investigations on ASR products extracted from concrete are difficult due to their small quantities. The extraction usually results in contamination with cement paste and/or aggregate constituents. Moreover, age and water content of the ASR products remain unknown. Hence, it was necessary to synthesize ASR products in sufficient amounts, of defined composition and to study them at different ages. The investigations include SEM/cryo-SEM studies, nanoparticle tracking analysis (NTA), ^{29}Si NMR and XRD analyses as well as water absorption measurements. For some of them, first results are presented.

2. MATERIALS AND METHODS

2.1 Synthesis of the ASR products

Based on about 400 SEM/EDS analyses of ASR products in concrete structures examined earlier and concrete prisms recently tested with the CS-CPT [2, 5], 4 main compositions were selected for the synthesis of the ASR products (Figure 2.1). One composition rich in alkalis (55-65 wt.% Na_2O+K_2O), one rich in SiO_2 (65 wt.%) and both of them with (10 wt.% CaO) and without Ca. Each of those 4 main compositions was used to prepare ASR products at 40 °C with a low (150 wt.% of the solid ASR product) and high (450 wt.% of the solid ASR product) water content. For the water content, assumptions had to be made, because the water content of real ASR products in concrete is unknown. Additionally, two ASR products were prepared at 60 °C for comparison, resulting in 10 different variants of synthetic ASR products (Table 2.1). For some of them, first results are presented.

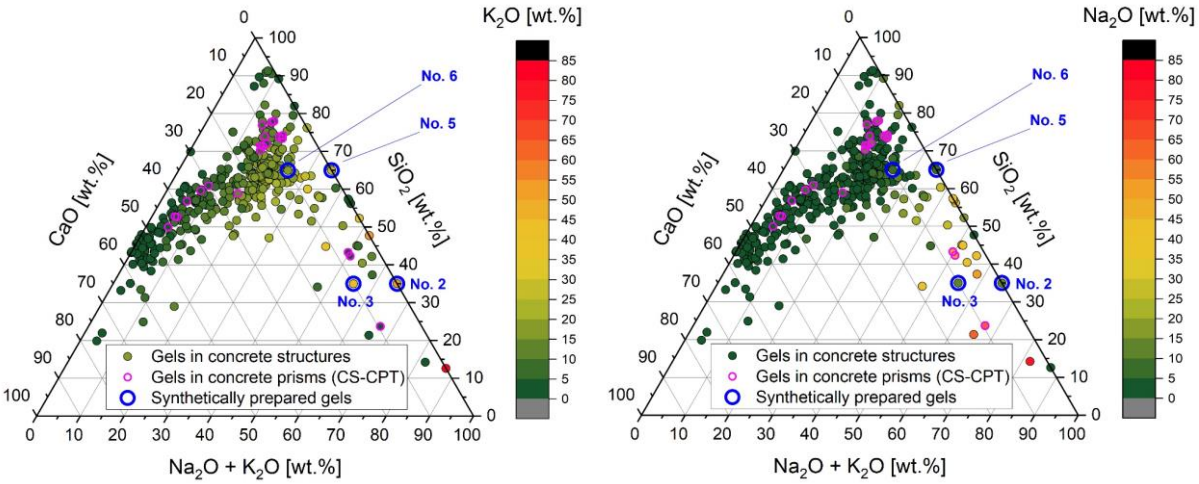

Figure 2.1: Composition (SEM/EDS) of ASR products in concrete structures, concrete prisms (CS-CPT) and as synthetically prepared (Table 2.1), left: K_2O distribution, right: Na_2O distribution

Table 2.1: Characteristic values (nominal) of the synthetic ASR products

No.	SiO_2	CaO	K_2O	Na_2O	H_2O*	Si	Ca	K	Na	T
[-]	[wt.%]	[wt.%]	[wt.%]	[wt.%]	[wt.%]	[mol/l]	[mol/l]	[mol/l]	[mol/l]	[°C]
2A	35.0	---	50.2	14.8	450	1.29	---	2.37	1.06	40
2C	35.0	---	50.2	14.8	150	3.88	---	7.11	3.18	40
3A	35.0	10.0	42.5	12.5	450	1.29	0.40	2.01	0.90	40
3C	35.0	10.0	42.5	12.5	150	3.88	1.19	6.02	2.69	40
3D	35.0	10.0	42.5	12.5	450	1.29	0.40	2.01	0.90	60
5A	65.0	---	27.0	8.0	450	2.40	---	1.27	0.57	40
5C	65.0	---	27.0	8.0	150	7.21	---	3.82	1.72	40
6A	65.0	10.0	19.3	5.7	450	2.40	0.40	0.91	0.41	40
6C	65.0	10.0	19.3	5.7	150	7.21	1.19	2.73	1.23	40
6D	65.0	10.0	19.3	5.7	450	2.40	0.40	0.91	0.41	60

* related to the dry mass of the solid ASR product

The ASR products were prepared by following the reaction sequence in concrete as close as possible. The required amounts of KOH (pellets ≥ 85 %, Merck) and NaOH (granules ≥ 98 %, Merck) were dissolved in de-ionized water at 40 and 60 °C respectively in a HDPE bottle (500 ml) while continuously stirred at 400 min^{-1} for 30 min by using a magnetic stirrer. Afterwards, SiO_2 (precipitated silicic acid,

extra pure heavy ≥ 99 %, surface area 16.8 m²/g, Merck) was added and the resulting slurry was further mixed continuously with an overhead stirrer at 1200 min^{-1} for 30-150 min until the silica had dissolved completely. For the ASR products with Ca, the final step was to add a slurry of $Ca(OH)_2$ into the derived alkali-silica sol while mixing with an overhead stirrer at 2000 min^{-1}. The slurry was prepared before by mixing the required amount of $Ca(OH)_2$ (powder ≥ 98 %, Merck) into a part of the total de-ionized water at a ratio of 1:3 at 400 min^{-1} for 30 min by using a magnetic stirrer. Attention was paid to add the $Ca(OH)_2$ slurry as quickly (< 1 s) as possible by injection with a syringe into the alkali-silica sol in order to ensure a uniform distribution of the $Ca(OH)_2$ prior to gelation. Gelation occurred quickly for the products rich in SiO_2 (6A: approx. 180 s, 6C: approx. 30 s after adding the $Ca(OH)_2$ slurry) and turned the sol into a highly viscous gel that could no longer be mixed. For the products rich in alkalis, the mixing was stopped 30 min after the $Ca(OH)_2$ slurry was added, but the gelation occurred considerably later (3A: approx. 60 min, 3C: approx. 45 min). All the HDPE bottles were sealed airtight and are kept at 40 and 60 °C respectively until the time of investigation after 1 day and 24, 48 and 72 weeks.

2.2 Scanning electron microscopy (SEM)

For the SEM analysis with energy-dispersive x-ray spectroscopy (EDS), the synthetic ASR products were prepared in two different ways to maintain their original structure as far as possible.

First, samples were cryogenically frozen in liquid nitrogen (-196 °C). Due to the instant freezing using a high-pressure (2100 bar) freezing unit (HPM100, Leica), the formation of ice crystals that would interfere with the SEM analysis is adequately suppressed. The samples are sandwiched-frozen between two copper shells (Ø 3 mm) that are subsequently fractured using a high vacuum preparation system (MED020, Leica). Afterwards, the samples are transferred into the pre-cooled SEM (Helios Nanolab G4 UXN, Thermo Fisher Scientific) using a cryo transfer shuttle system (EM VCT500, Leica). During the examinations, the samples were heated stepwise under high vacuum conditions (1.5-4 kV, 6-100 pA) from -140 to -70 °C, resulting in the sublimation (transition from solid into gas) of the amorphous ice.

Second, samples were prepared by critical point drying. The liquid phase of the samples was exchanged against acetone by multiple rinsing. The rinsed samples were placed in a pressure chamber at 15 °C and approx. 50 bar while the chamber was flushed several times with liquid CO_2 to remove the acetone from the samples. Afterwards, the temperature was increased to 35 °C at 100 bar, exceeding the critical point of CO_2 (31 °C at 74 bar), i.e. there is no difference between the liquid and gaseous state of CO_2 anymore. By slowly releasing the CO_2, the samples largely maintain their original structure since no capillary forces occur as for normal drying due to passing the liquid/gas phase boundary. Afterwards, the samples were examined in the SEM (FEI, NOVA™ NanoSEM 230) in high-vacuum mode at 2-5 kV and 4-130 pA.

2.3 Nanoparticle tracking analysis (NTA)

The ASR products were studied microscopically while exposed to laser light (λ = 638 nm, red) in the NTA device (NANOSIGHT LM10). In order to obtain a particle concentration within the operating conditions, it was necessary to dilute the samples up to a total water content of 1350 % for the ASR products free of Ca and 5400 % for the ones with Ca. The diluted samples were injected into the laser chamber, between an aluminium body and a special glass plate. Particles with a size of 10-1000 nm become visible due to their scattering of the laser light (TYNDALL effect), allowing to track their continuous BROWNian motion. A camera, attached to the microscope, records short (60 s) video sequences of the particle motion that is automatically tracked and analysed by a software based on the STOKES-EINSTEIN equation, allowing to estimate the particle size distribution. In order to increase the precision, for every sample 6 video sequences were recorded and the average result was obtained.

2.4 Osmotic cell test (OCT)

The osmotic water absorption of the synthetic ASR products was determined by filling a sample (5 ml) of the ASR products into a cut PP vial (50 ml) onto a track-etched polycarbonate membrane with a pore size of 100 nm immersed in de-ionized water. The membrane was placed into the perforated vial cap that was tightly screwed to the vial. The vial was immersed 5-8 mm upside down in a bath of de-ionized water at 20 °C, by placing the perforated vial cap on a spacer that allows the water to fully access the membrane. The sample of the ASR product was applied directly onto the membrane through the cut bottom of the vial. The filling level of the vial was monitored until no further change occurred.

3. RESULTS AND DISCUSSION

3.1 Synthesis of the ASR products

Shortly after the synthesis, the ASR products free of Ca (sol) were clear and of low viscosity while all the ASR products with Ca (gel) appeared opaque/white and were much more viscous (Figure 3.1), ranging from jelly-like (3A) to crumble-like (6C). In general, the viscosity of the ASR products increased with a higher silica content, a lower alkali and water content as well as by adding Ca. First, the ASR products free of Ca appeared clear but already showed the TYNDALL effect when exposed to laser light what confirms the presence of colloidal particles. Over time, the appearance of the ASR products started to change. The ones free of Ca and especially those low in water content (150 wt.%) showed an increasing cloudiness and intensified TYNDALL effect (Figure 3.2), while some of the ASR products with Ca (esp. 3C) started to change their colour from white into light yellow/brown.

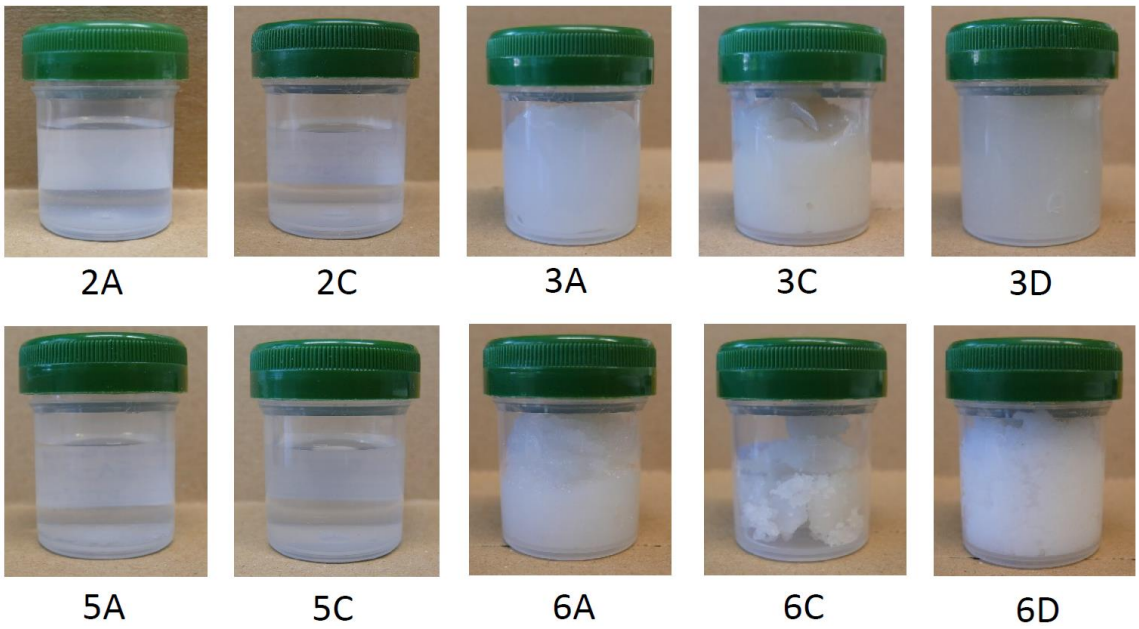

Figure 3.1: Appearance of the ASR products (Table 2.1), 1 day after the synthesis

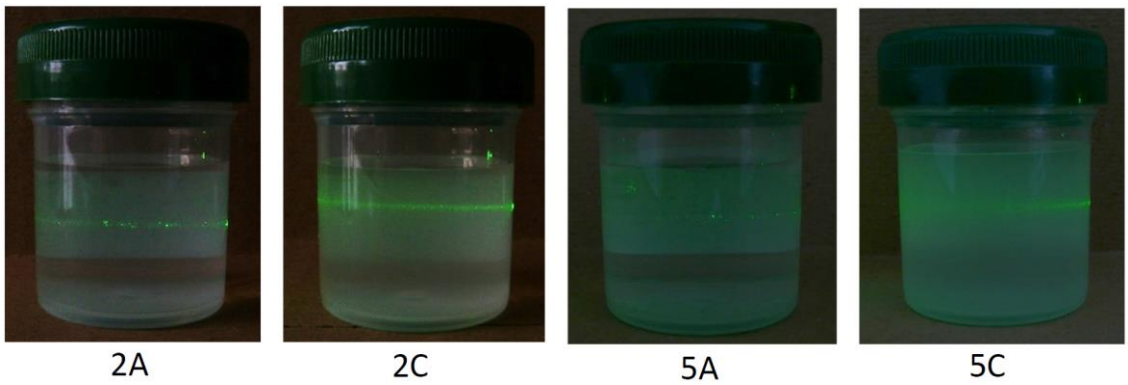

Figure 3.2: ASR products free of Ca after 24 weeks of ageing at 40 °C showing the TYNDALL effect when exposed to laser light (λ = 532 nm)

3.2 Scanning electron microscopy (SEM)

Most of the ASR products could be studied best when prepared with critical point drying, since the free solution, even if frozen, disturbs the SEM analysis and is removed by this method. Only for some of the ASR products with Ca, structural details could be studied better in the frozen state.

The ASR product 2A (Figure 3.3), rich in alkalis and free of Ca, appeared homogenous and structureless after 1 day when frozen but a coarsening and the development of fractal-like structures was evident after 12 weeks [6, 7]. After some more time (24 weeks), filament-like structures became evident after sublimation with a thickness of 20-100 nm and a length of 300-1000 nm (Figure 3.4). The ASR product 5C (Figure 3.5), rich in Si and free of Ca, showed a matrix of particles after critical point drying with a size of 60-500 nm and irregular shape.

The ASR product 3A, rich in alkalis and with Ca, showed particles with a size of 50-150 nm in nearly spherical shape, embedded in a dense matrix (Figure 3.6). The ASR product 6C (Figure 3.7), rich in silica and with Ca, showed a fine pored sponge-like structure with embedded platelet-like phases of µm-size that resemble the platelets known from rosette type ASR products. A sponge-like structure was evident in all ASR products with Ca and could be identified best in the frozen state, after the sublimation of the amorphous ice. For ASR product 6A, the pore size of the sponge-like structure was between 30-150 nm (Figure 3.8).

Overall, the ASR products free of Ca contain particles of colloidal size and not necessarily of spherical shape. Mainly due to their small size, the composition of the particles could only be determined roughly by EDS analysis but they all showed Na, K and Si as expected. The ASR products with Ca showed a sponge-like structure of different fineness (depending on the water content) and embedded particles of colloidal size as well as larger platelet-like phases containing more Si than the surroundings.

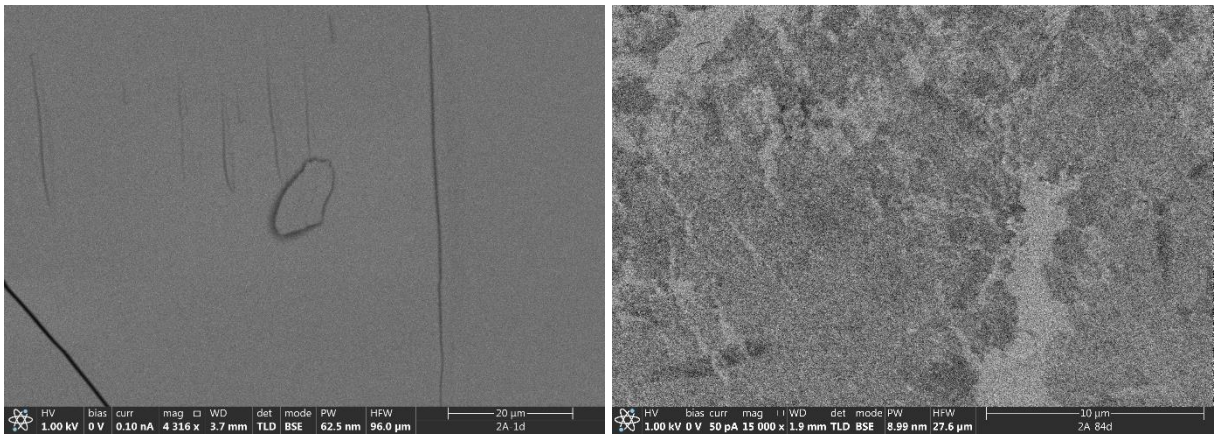

Figure 3.3: ASR product 2A (cryogenically frozen), structureless after 1 day (left) and with fractal-like structures after 12 weeks of ageing at 40 °C (right), [6]

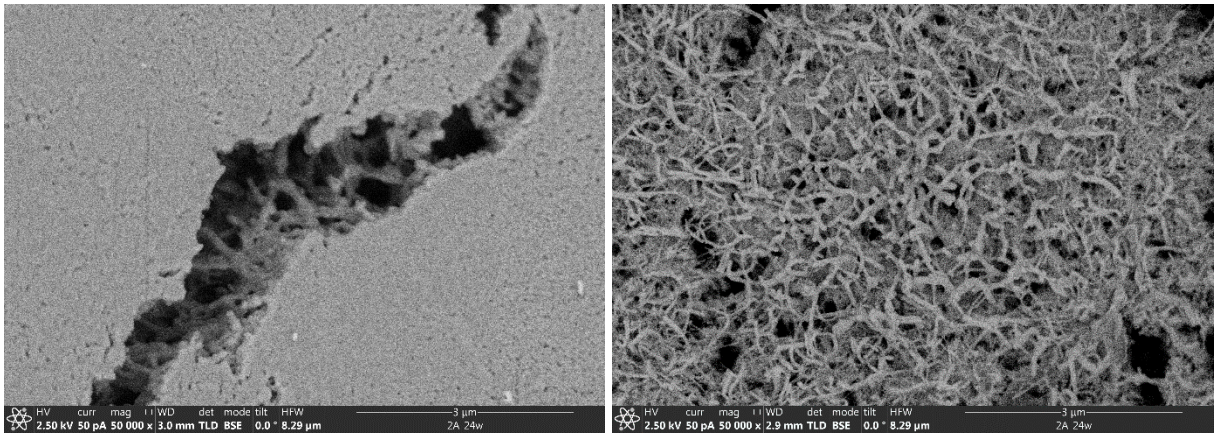

Figure 3.4: ASR product 2A (cryogenically frozen, after sublimation to -80 °C) showing a matrix of filament-like particles after 24 weeks of ageing at 40 °C

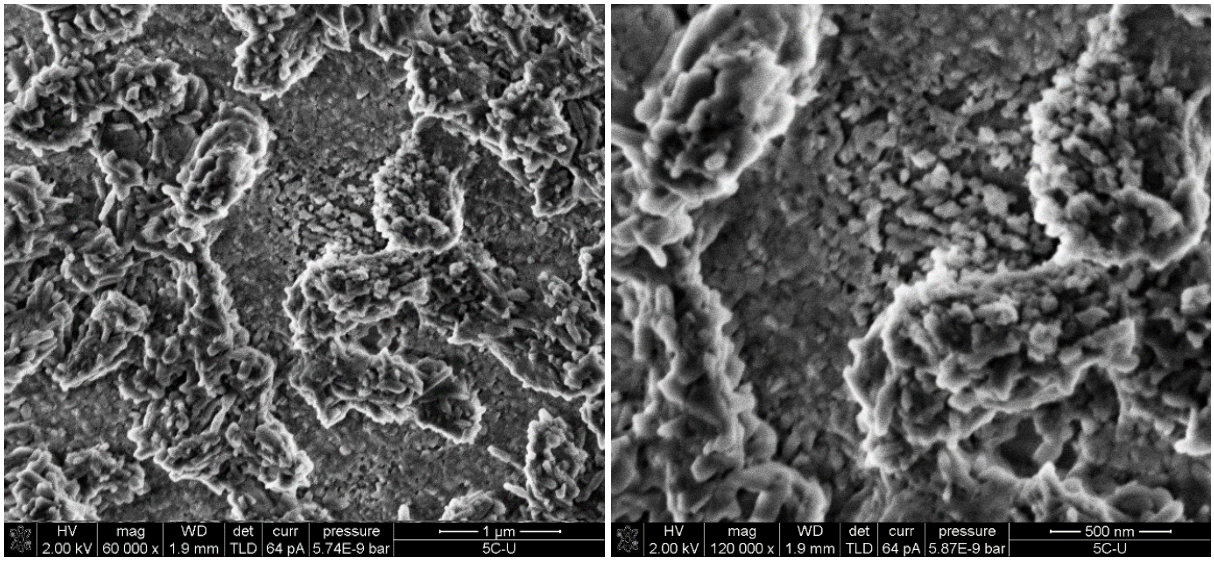

Figure 3.5: ASR product 5C (critical point drying) showing a matrix of particles with a size of 60-500 nm after 24 weeks of ageing at 40 °C

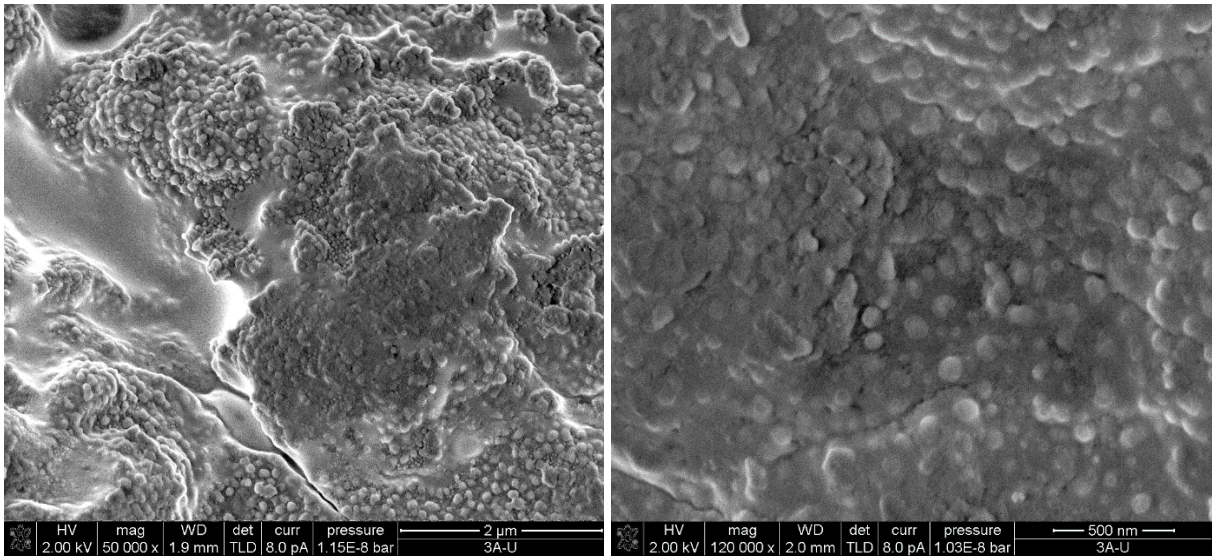

Figure 3.6: ASR product Gel 3A (critical point drying) showing particles with a size of 50-150 nm in a dense matrix after 24 weeks of ageing at 40 °C

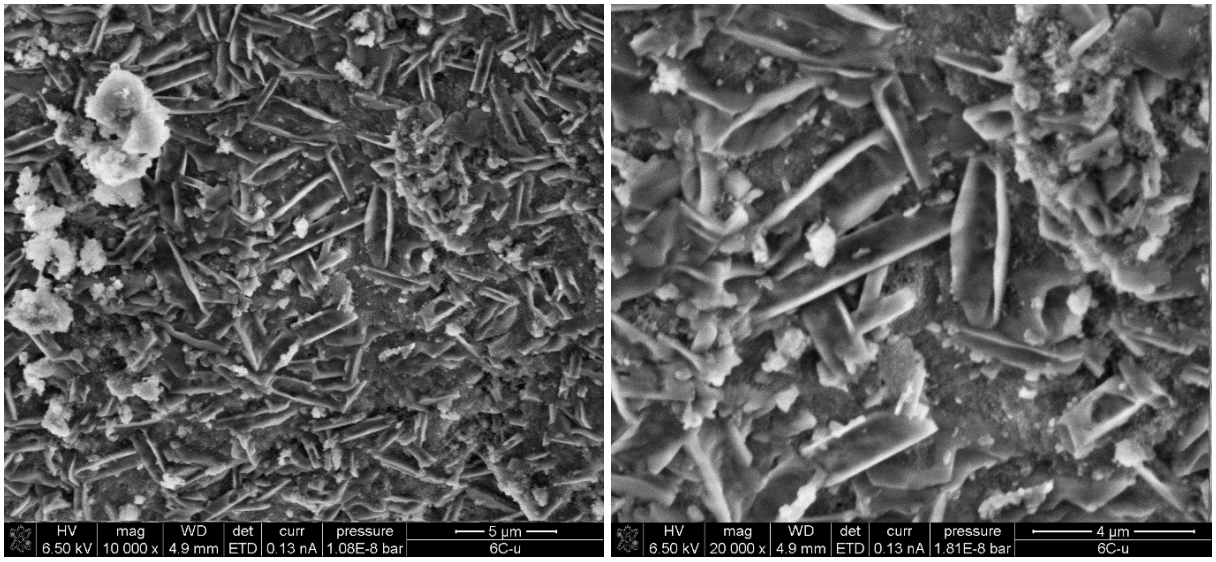

Figure 3.7: ASR product 6C (critical point drying) showing platelet-like phases of µm-size and rich in Si after 24 weeks of ageing at 40 °C

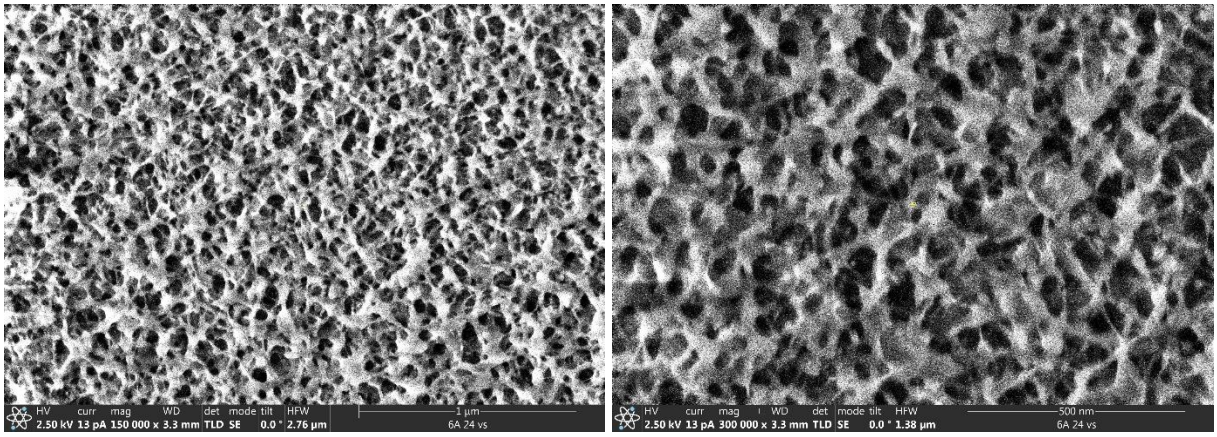

Figure 3.8: ASR product 6A (cryogenically frozen, after sublimation to -110 °C) showing a sponge-like structure with a pore size of 30-150 nm after 24 weeks of ageing at 40 °C

3.3 Nanoparticle tracking analysis (NTA)

The NTA for the ASR products free of Ca clearly showed particles with a size between 50-600 nm in continuous BROWNian motion (Figure 3.9). In general, the particle concentration increase with the Si concentration in the ASR products (Figure 3.10, left), although inaccuracies due to dilution and probably agglomeration effects may reduce the quality of the correlation. The ageing of the ASR products is still in progress, but first result indicate that larger particles are formed from those of smaller size (OSTWALD ripening) in the ASR products free of Ca after storage at 40 °C for 24 weeks (Figure 3.10, right).

For the ASR products with Ca, blurry and irregular shapes instead of clearly defined particles appeared in the microscope. Mixing (5 min at 500 min^{-1}) and ultrasonic bath treatment (15 min at 35 kHz) does not result in re-dispersion. Hence, the NTA cannot be applied for those ASR products. Obviously, the addition of Ca resulted in a largely and irreversible aggregation of the colloidal particles in the former silica sol.

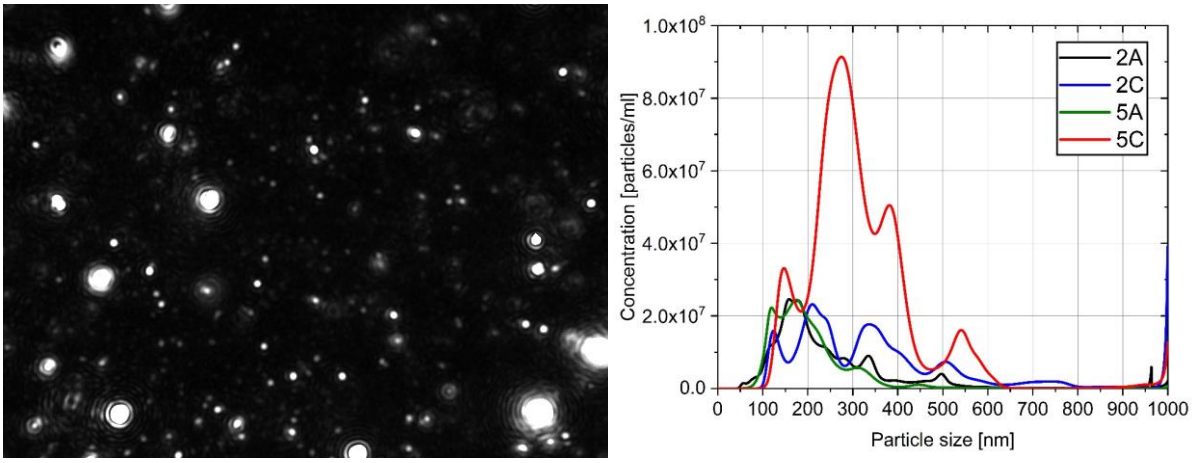

Figure 3.9: NTA image with clearly defined particles (scale bar not available) in ASR product 5C (left) and particle size distribution for the ASR products free of Ca after 24 weeks of ageing at 40 °C (right)

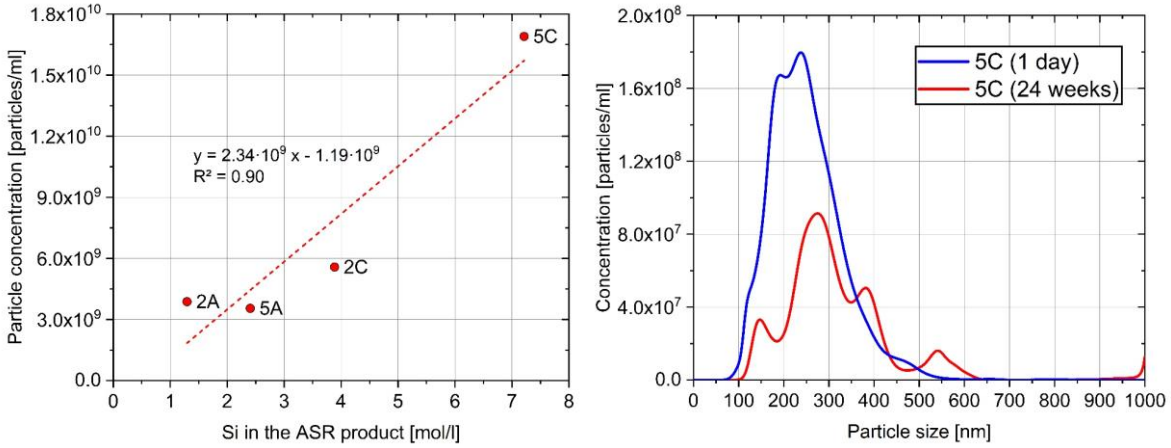

Figure 3.10: Correlation between Si concentration and total particle concentration in the the ASR products (left) and particle size distribution in ASR product 5C after 1 day and 24 weeks (right)

3.4 Osmotic cell test (OCT)

In the OCT, all the ASR products free of Ca showed an increase of the filling level within a few hours up to 320 vol.%, while the ASR products with Ca did not change their volume over a period of several days (Figure 3.11). A comparison between the highest volume increase and the total Si concentration of the ASR products free of Ca (Table 2.1) showed a strong correlation (Figure 3.12).

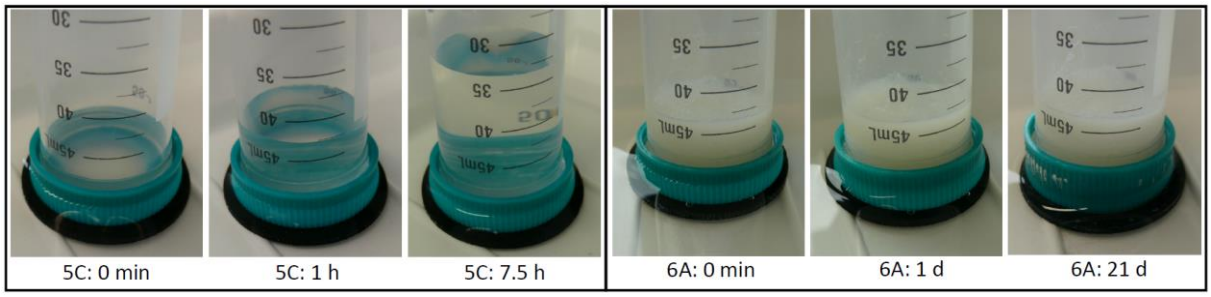

Figure 3.11: Osmotic cell test for ASR product 5C, free of Ca (left) after 0 min, 1 h and 7.5 h (from left to right) and ASR product 6A, with Ca (right) after 0 min, 1 day and 21 days (from left to right)

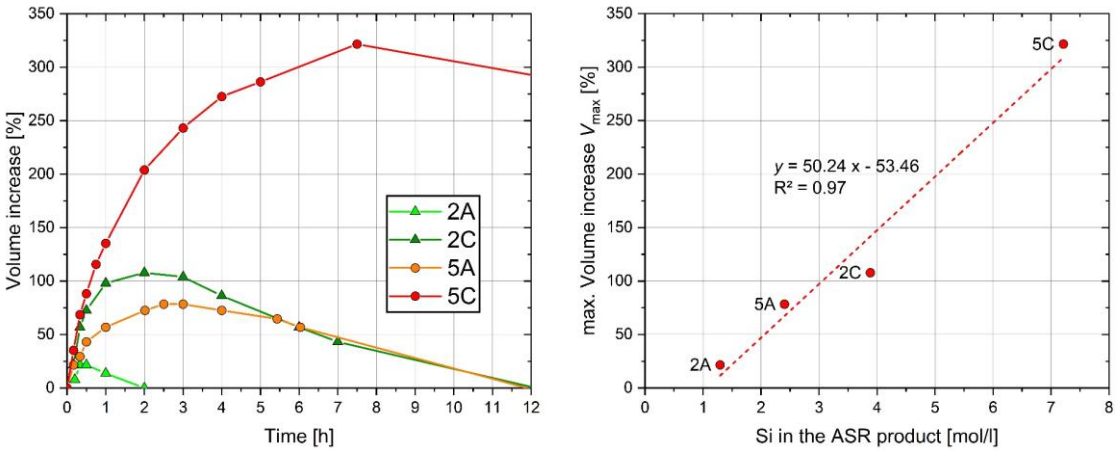

Figure 3.12: Volume increase in the osmotic cell tests for the ASR products free of Ca (left) and comparison between the highest volume increase and the Si concentration in the ASR products (right)

Classic osmosis occurs when a membrane between a solution and its pure solvent is permeable only to the solvent, often water. Because the chemical potential of the water in the solution is less than that of the pure water, the pure water will pass through the membrane into the solution in order to equilibrate the chemical potentials by diluting the solution. A pressure applied to the solution that precisely prevents the pure water from flowing though the membrane is called the osmotic pressure and can be calculated using the VAN'T HOFF equation for ideal (diluted) solutions or based on the activity of the water for non-ideal (concentrated) solutions [8].

The situation is more complex, if there is a solution of certain composition on both sides of the membrane and/or if the membrane is not only permeable to water but to some of the dissolved ions. This results in an unequal distribution of the ions on both sides of the membrane, since the ions unable to permeate are forced to stay on one side of the membrane while simultaneously, the solutions on both sides of the membrane remain electrically neutral. Because the resulting total concentration is higher on the side with the ions unable to permeate, osmosis occurs and water flows to this side. This effect was described by DONNAN in 1911 and was applied later to colloids, for which the colloidal particles are the ones unable to pass the membrane [3, 9]. The resulting osmotic pressure in such systems is the difference between the osmotic pressures for the solutions of either side of the membrane [3, 4, 9].

For the osmotic cell tests in this study, the membrane is permeable to water, all the ions (Na^+, K^+, Ca^{2+}, OH^-, monomeric silica) as well as particles of a size < 100 nm but impermeable to particles > 100 nm. A volume increase occurred only for the ASR products free of Ca, since they contain freely movable particles of that size (≥ 100 nm) as shown before (SEM, NTA). The use of a membrane with a pore size of 1000 nm instead of 100 nm did not result in a volume increase for the very same ASR products. The higher the Si concentration in the ASR products, the higher the volume increase, because the osmotic pressure depends on the number of the osmotically active compounds what are the colloidal alkali-silica particles in this case, based on the DONNAN effect.

After reaching the maximum volume, the filling level in the osmotic cells decreased gradually for all the ASR products free of Ca (Figure 3.12). During the osmotic cell tests, the formation of fine fractal-like clusters occurred, probably caused by aggregation of colloidal particles what would lower the osmotic activity and possibly resulted in the backflow of solution.

3.5 Transfer of the results to ASR in concrete

The mechanism of expansion caused by ASR was explained first 1944 by HANSEN based on the osmotic pressure hypothesis [10]. However, the existence of a semi-permeable membrane in concrete, as required for osmosis, was often questioned. The absorption theory, which explains the swelling of the ASR product due to water imbibition, was more widely accepted later on. Based on the first preliminary results in this study, however, it is likely that colloidal alkali-silica particles are unable to pass pores in aggregate grains and the cement paste that are smaller than themselves, representing a mechanism of semi-permeability that results in osmosis. This mechanism, if transferred to concrete, could extend the understanding of the ASR approximately as follows (Figure 3.13):

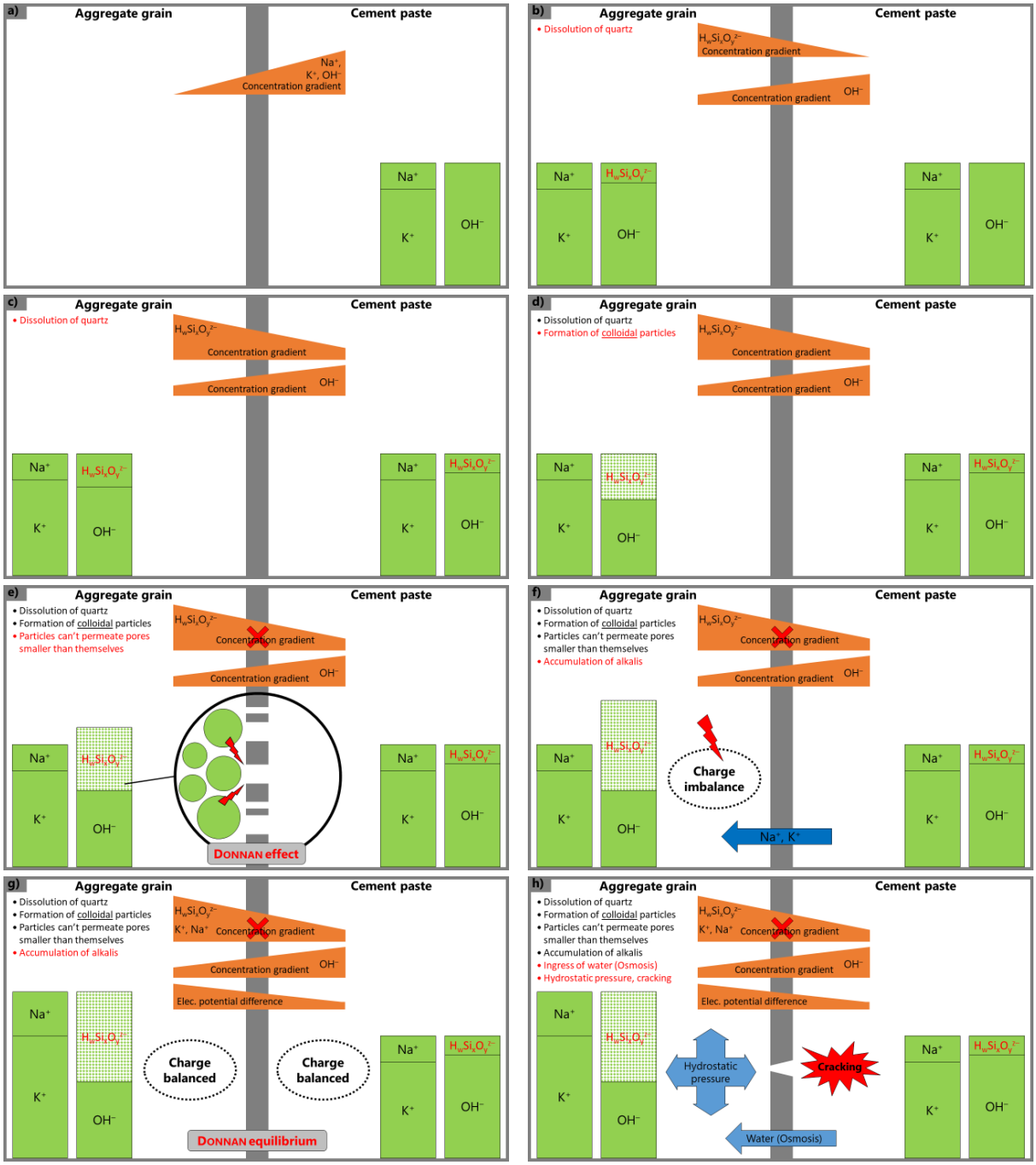

Figure 3.13: Simplified transfer of the colloidal effects of ASR products free of Ca to ASR in concrete

a) First, the concentration gradient between the pore solution in the cement paste and in an alkali-reactive aggregate grain result in diffusion of the ions (mainly K^+, Na^+, OH^-) into the grain in order to reach an equilibrium.
b) In the aggregate grain, OH^- ions start to dissolve silica by breaking up siloxane (Si-O-Si) bonds. OH^- ions are consumed and silica species ($H_wSi_xO_y^{z-}$) are released, resulting in concentration gradients between the solutions in the aggregate grain and the cement paste.
c) At the beginning of the silica dissolution, the low silica concentration in the solution of the grain results in monomeric silica species as $H_2SiO_4^{2-}$ that are still able to diffuse out of the grain. In the opposite direction, new OH^- ions diffuse into the grain.
d) The further dissolution of the silica results in a gradual increase of the silica concentration in the solution of the grain, leading to more complex, polymeric silica species and finally colloidal particles start to form. Over time, number and size of the colloidal particles increase.

e) At some point, number and size of the colloidal particles reach a state that prevent most of them from leaving the grain and/or diffusing through the cement paste (DONNAN effect). Since the pore size (diameter) of mature cement pastes is mainly in the range of 3-100 nm, especially particles ≥ 100 nm are unable to move through the cement paste.
f) In order to maintain the solution electrically neutral, positively charged ions have to enter the grain in order to balance the negatively charged colloidal silica particles, what results in the accumulation of alkalis. Since alkalis are available in much larger quantity in the concrete pore solution than Ca, at first the ASR products are free or poor in Ca.
g) Besides the concentration gradients, an electrochemical potential difference (DONNAN potential) develops between the solution in the aggregate grain and in the cement paste. Individually, however, both solutions are charge balanced (DONNAN equilibrium). The colloidal alkali-silica product is unable to leave the grain and/or move through the cement paste.
h) Because now, the chemical potential of the water in the grain (ASR products) is less than that of the surrounding water in the cement paste (pore solution), water flows osmotically driven into the grain (dilution flow). Consequently, a hydrostatic pressure develops, possibly able to crack the grain and/or the cement paste at some point.

A strong indication that the DONNAN effect is of relevance in concrete is the accumulation of alkalis opposite to diffusion flow, which results in a much higher alkali concentration in the ASR products than in the concrete pore solution. Whether the hydrostatic pressure would be high enough to cause cracking in concrete, requires verification. In general, the osmotic pressure for colloids is smaller than for true solutions, because the number of the osmotically active colloidal particles is low compared to dissolved ions [3, 4]. However, the colloidal particles are physically unable to pass any pores with a size smaller than their own. Therefore, the DONNAN effect is not necessarily restricted to the ITZ as simplified illustrated in Figure 3.13 but may also occur within the aggregate grain, the hardened cement paste or both. Hence, a multitude of osmotic cells would be possible to form in and around alkali-reactive aggregate grains, which in total could lead to critical pressures.

Once the ASR products free or poor in Ca get in contact with larger amounts of Ca, as in the cement paste (portlandite) or high volumes of pore solution, gelation occurs. The colloidal particles start to aggregate irreversibly (coagulation) and are no longer osmotically active, forming Ca-containing ASR products, obviously less or non-expansive and possibly transformed into thermodynamically more stable crystalline products over time as often found in concrete [11]. If ASR products with less Ca (< 10 wt.% CaO) or water (< 150 wt.%) show a different swelling behaviour or at which amount of Ca or water the aggregation starts respectively needs to be clarified.

4. CONCLUSIONS

Based on a number of earlier observations, it appeared that ASR products could be considered as colloidal systems. In order to clarify, if and to what extent ASR products exhibit colloidal properties, 10 ASR products of different composition, water content and prepared at different temperatures have been synthesized and are currently under investigation. First and preliminary results show that:

- ASR products free of Ca contain freely movable colloidal particles with a size of 50-600 nm.
- The colloidal particles are unable to pass pores with a size smaller than their own, representing a mechanism of semi-permeability (DONNAN effect) that results in osmosis.
- With increasing Si concentration in the ASR product, the particle concentration and the osmotic effect increases.
- Over time, there is a process of ageing, resulting in the decrease of the particle concentration, the increase of the particle size and in aggregation as the formation of fractal-like structures.
- By adding Ca (10 wt.% CaO), the colloidal particles coagulate irreversibly and form larger clusters of sponge-like structures with embedded particles of colloidal size as well as larger, platelet-like phases.
- Currently, the studied ASR products with Ca (10 wt.% CaO) do not show osmotic swelling.

5. ACKNOWLEDGEMENTS

The author gratefully acknowledge the German Research Foundation (DFG) for the financial support of this study (GI 1369/2-1), Christiane Rößler (Cryo-SEM), Bernd Möser (SEM) and Steffen Hausdorf (critical point drying, TU Dresden) for the technical support as well as Katrin Seyfarth for the review of the manuscript.

6. REFERENCES

[1] Giebson C, Seyfarth K, Ludwig HM (2021) Aggregate dissolution kinetics. In: Batista AL, Santos Silva A, Fernandes I, Oliveira Santos L, Custódio J, Serra C (eds.): Proceedings of the 16th ICAAR, Vol. 1, Lisboa, Portugal, 161-173

[2] Iskhakov T, Giebson C, Timothy JJ, Ludwig HM, Meschke G (2021) Deterioration of concrete due to ASR: Experiments and multiscale modeling. Cem Concr Res 149. https://doi.org/10.1016/j.cemconres.2021.106575

[3] Zsigmondy R (1925) Kolloidchemie. 5. Auflage, Otto Spamer Verlag, Leipzig

[4] Everett DH (1988) Basic principles of colloid science. The Royal Society of Chemistry

[5] Giebson C, Voland K, Ludwig HM, Meng B (2017) Alkali-silica reaction performance testing of concrete considering external alkalis and preexisting microcracks. Structural Concrete 18:528-538

[6] Hernandez L (2020) Investigations into the ageing behaviour of ASR gels. Master Thesis, Bauhaus-University Weimar

[7] Wijnen, PWJG (1990) A spectroscopic study of silica gel formation from aqueous silicate solutions. Technische Universiteit Eindhoven. https://doi.org/10.6100/IR342612

[8] Levine IN (2009) Physical chemistry. McGraw-Hill, 6th International Edition

[9] Yartsev A (2013) Deranged Physiology. https://derangedphysiology.com

[10] Hansen WC (1944) Studies relating to the mechanism by which alkali-aggregate reaction produces expansion in concrete. ACI Journal Proceedings 40:213-227

[11] Katayama T (2012) ASR gels and their crystalline phases in concrete – Universal products in alkali-silica, alkali-silicate and alkali-carbonate reactions. In: Drimalas T, Ideker JH, Fournier B (eds.): Proceedings of the 14th ICAAR, Austin, Texas, USA, 12 pp.